J Mater Sci: Mater Electron (2022) 33:16511–16520

The effect of Lissamine fast yellow dye intercalation into Zn/Al layered double hydroxides on the mechanical and thermal properties of poly(vinyl chloride)

Negar Roghani[1], Mohammad Dinari[1,*], and Ehsan Tolouei[1]

[1] *Department of Chemistry, Isfahan University of Technology, Isfahan 84156-83111, Islamic Republic of Iran*

Received: 5 March 2022
Accepted: 7 June 2022
Published online: 11 June 2022

ABSTRACT

In the present work, Zn/Al layered double hydroxide (LDH) was modified by Lissamine fast yellow by the co-precipitation method. Infrared spectroscopy and X-ray diffraction pattern studies showed the presence of Lissamine fast yellow anion between LDH layers. After identifying, poly(vinyl chloride) (PVC)-based nanocomposites were prepared by soluble processing method under ultrasound waves by adding three different percentages of synthesized LDH as a thermal stabilizer and their effect on the mechanical and thermal properties of PVC was investigated. Then, the structure and morphology of the resulting nanocomposites were investigated by infrared spectroscopy, X-ray diffraction pattern, scanning electron microscope, and transmission electron microscopy. The results of electron microscopy showed a relatively uniform distribution of synthesized nanoparticles in the polymer matrix. Based on the thermal stability analysis performed, the char yield of the nanocomposites has expanded compared to pure PVC residues. Also, the limiting oxygen index has increased by about 45%. The mechanical strength ratio of nanocomposite significantly increased in comparison to pure PVC. In this research, an attempt has been made to synthesize a new substance that acts as a thermal stabilizer and also as a pigment.

1 Introduction

One of the most common, strong, but lightweight thermoplastics used in industrials is poly(vinyl chloride) (PVC) [1–3]. Due to its unique properties, it has many industrial applications. It is possible to combine PVC with various additives for special purposes; this process is called compounding [4]. Some additives may affect the PVC composites parameters, such as mechanical properties, thermal stability, color, and other items, which cause using PVC composite in the flexible application makes it such a highly versatile polymer [2–4]. The most important additives that are applied in PVC composites contain lubricants, thermal stabilizers, and sometimes plasticizers [2, 5–7]. Selective additives

Address correspondence to E-mail: mdinary@gmail.com; dinari@iut.ac.ir

https://doi.org/10.1007/s10854-022-08544-8

include several substances like processing aids, flame retardants, thermal and impact modifiers, UV stabilizers, fillers, pigments, and blowing agents for defined applications [6]. Fire retardant is one of the principal properties of PVC and that is why the chlorine in the PVC substrates; however, some additives could improve this property of the PVC [8–10]. Due to arrest the decomposition of the PVC by heat using heat stabilizers is required and necessary in all production PVC formulations. Heat stabilizers also can intensify the PVC's resistance to daylight, weathering, and heat aging [11]. Furthermore, they have a critical impact on the physical properties of the PVC and the cost of the formulation [11–13]. As mentioned before, another additive used in PVC compounds is pigmented. Pigments used for PVC must be stable in terms of thermal and light and suitable disability, and they should be matchable with the formulation. Mineral pigments are more commonly used in industry. It may also be necessary to follow certain rules to use them in cases related to children's food and toys, etc. [14–16].

Layered double hydroxides (LDHs) are biocompatible inorganic nanomaterials that also have a layered structure. These nanoparticles can play the role of thermal stabilizer for PVC [17]. Their structure has several layers and the layers that make up these nanoparticles are positively charged, and there are anions and water molecules between the layers. These layers and interlayer anions are connected by electrostatic interaction [17–19]. LDHs have an intrinsic hydrogen chloride (HCl) absorption capacity and thus can improve the thermal stability of PVC. Recently, the addition of LDHs to the PVC matrix to prepare PVC/LDH nanocomposites (NCs) has attracted much interest. For example, Gao et al. have studied the effect of Co/Al-LD and modified Co/Fe-LDH on PVC and they concluded that the synthesized LDHs increased the thermal stability and reduced the heat loss of PVC composites at high temperatures and that the emissions of toxic gases such as CH_4, CO, and NO_x were reduced by both LDHs [20–23]. Kang et al. use a new method to transfer low flammability to LDH/polymer-based composites [24]. In their study, dye structure-intercalated LDH was prepared and its effect on the flammability of polypropylene-grafted maleic anhydride/LDH was investigated. The results demonstrated that dye structure-intercalated LDH decreases the heat release rate and the total heat release of the resulting composite [25, 26].

In our recent work, triazine-based modified Zn–Al-LDH was prepared to increase the thermal and mechanical stability of PVC. It has been observed that at 800 °C, the amount of nanocomposite remaining is 70% higher and more mechanical strength has been observed [27]. Lissamine (Lis) fast yellow dye is extensively used in food, textile, and leather industries as a colorant [28, 29]. In this study, Lis was used as an interlayer anion to prepare modified zinc/aluminum LDH nanoparticles by the co-precipitation method. After characterization of Lis-modified layered double hydroxide (Lis-LDH), it was used as both thermal stabilizers and pigments for PVC products. Finally, the mechanical and thermal properties of the prepared NCs are investigated.

2 Experimental

2.1 Chemicals

Lissamine fast yellow dye (I) was bought from Sigma-Aldrich company. Zinc nitrate hexahydrate, aluminum nitrate nonahydrate, sodium nitrate, and tetrahydrofuran (THF) were purchased from Merck CO. PVC grade is s6558 and it was used for the preparation of the NCs.

2.2 Synthesis of Lis-LDH

For the synthesis of Lis-LDH, 2 mmol of zinc nitrate. 6 H_2O, 1 mmol of aluminum (III) nitrate. 9 H_2O, and 1 mmol of yellow Lissamine were dissolved in 30 ml of deionized water in a two-necked round bottom. Then 10 mL of sodium hydroxide 2 mol/L was added slowly until the pH reaches 10 under a nitrogen atmosphere at 50 °C and stirred for 2 h. The contents were then transferred to an autoclave reactor and placed in an oven at 100 °C for 1 day. After that, the filtered precipitate was washed many times with ethanol and deionized water and dried for 24 h at 50 °C.

2.3 Preparation of the Lis-LDH/PVC films

Figure 1 shows the preparation of Lis-LDH/PVC NC films containing 4, 8, and 12% of Lis-LDH. First 1 g of PVC powder was dissolved in 10 mL of THF and

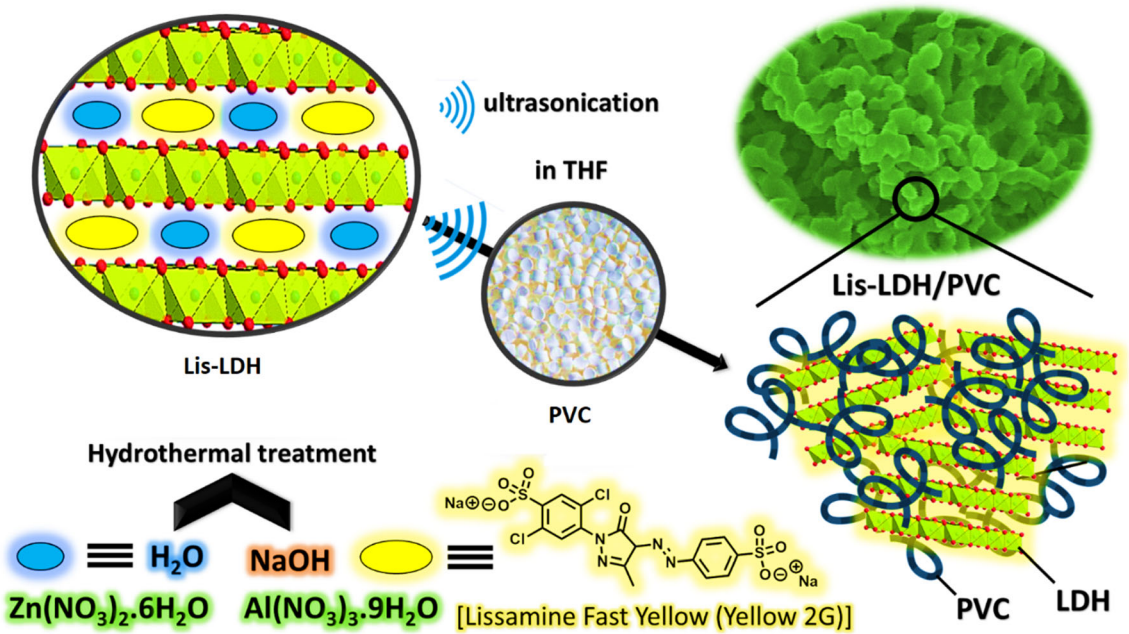

Fig. 1 Preparation of Lis-LDH/PVC NCs

then different amounts of Lis-LDH (4, 8, and 12% by weight of pure PVC) were dispersed in THF by sonication (SonoSwiss SW 3 H ultrasonic bath, Switzerland). In the next step, it was added to the polymer solution. The resulting mixture was then sonicated again and stirred for 2 h. The prepared homogeneous mixtures were gently poured into a petri dish to dry at ambient temperature [30].

2.4 Characterization techniques

To check the functional group of the Lis-LDH and NCs, FT-IR spectra (Jasco-680) were used. XRD was performed on a Bruker Nanostar X-ray powder diffractometer equipped with a

Cu Kα radiation at wavelength λ = 0.1542 nm and a generator working at 45 kV and 100 mA. A MIRA III FE-SEM and EDX were used for the morphology and topography of synthesized LDH and its NCs. TEM analysis was performed on Philips CM 120 microscope. An STA503 TA has been used to scrutiny the heat stability of NCs from 30 to 800 °C at the rate of 10 °C min^{-1} under the argon atmosphere. A Testometric Universal Testing Machine M350/500 (UK) was used for tensile testing at the rate of 5 mm/min. Samples were prepared with 40 mm * 10 mm with a thickness of 40 µm. At least 3 samples were examined for each type of NCs.

3 Results and discussion

3.1 FT-IR study

Figure 2 shows the FT-IR spectrum of Lis-LDH, PVC, and its NCs. For Lis-LDH, the absorption bands are in the range of 3428 and 3253 cm^{-1}, corresponding to the vibration of the hydroxyl groups on the layers, and the vibration of N–H of the Lissamine anions. Absorption bands at 1666 and 1501 cm^{-1} are attributed to the vibration of the C=O group and the vibration of the phenolic groups of the Lis. It is observed that the vibration of the SO_3 group was decreased at about 1155 and 1040 cm^{-1} due to the hydrogen bonding with OH group of LDH, and the C–Cl absorption band appears at 1620 cm^{-1}. Phenyl ring bonds are found in 700–900 cm^{-1}, C=C in 1600–1400 cm^{-1}, and $–CH_3$ in 1368 cm^{-1} [31, 32]. These results confirmed the formation of Lis-LDH. In the FT-IR spectra of neat PVC, the absorption bands at the range of 2800–3100 cm^{-1} and 1430 cm^{-1} show stretching bonds of –CH and CH–Cl, respectively. The vibration stretching of C–Cl in the syndiotactic and isotactic PVC structures is attributed to 614 cm^{-1} and 695 cm^{-1} bands [33, 34]. In the produced NC films, the absorption bands of the polymer and the nanoparticles are shown simultaneously. It has also been observed that with the increase of the

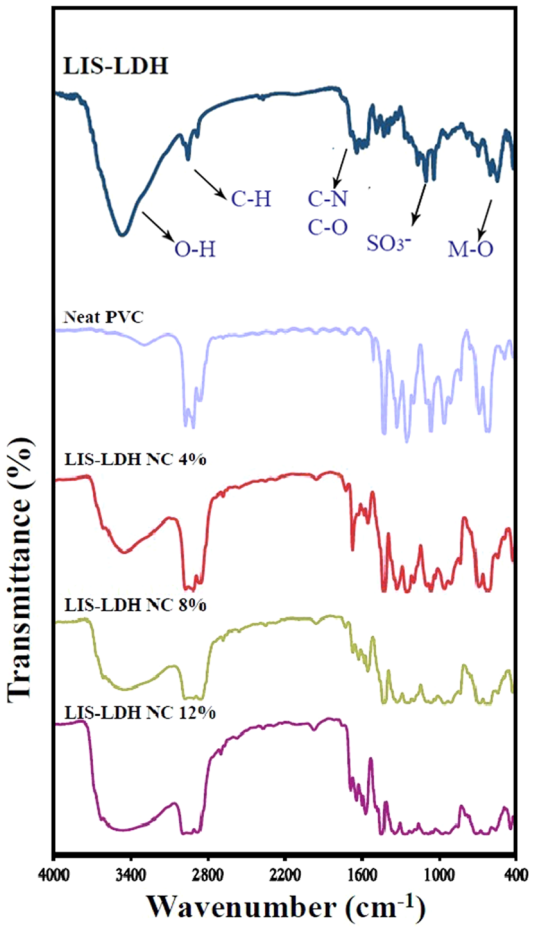

Fig. 2 FT-IR spectra in KBr pellet of Lis-LDH and the FT-IR at thin film of PVC and Lis-LDH/PVC NCs

nanoparticles in the polymer matrix, the Lis-LDH peaks intensify [35].

3.2 XRD analysis

XRD patterns of LDH, Lis-LDH, PVC, and NC 12 wt% are shown in Fig. 3. Specific absorption peaks at 2Θ=10, 21, 37°, (003), (006), and (009) indicate that Lis-LDH has a layered structure. These peaks are sharp, narrow, and symmetrical, indicating that the specimen is crystalline. The distance between the two layers was calculated to be 0.64 according to Bragg's law [13, 32]. Neat PVC film shows a large amorphous peak and by adding synthetic nanoparticles to the PVC polymer texture (in the 12 wt% of NC), the amorphous peak is still observed, but most of the original LDH peaks have been removed due to uniform distribution.

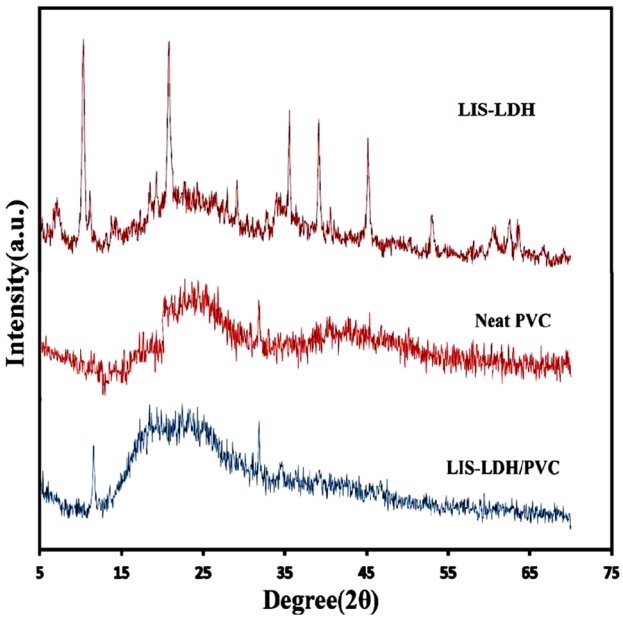

Fig. 3 XRD patterns of Lis-LDH Powder, neat PVC, and Lis-LDH/PVC NC 12 wt%

3.3 Thermal properties

The thermal properties of Lis-LDH, PVC, and NCs were examined up to 800 °C and are shown in Fig. 4. It should be mentioned that Lis-LDH nanoparticles at the temperature of 800 °C, about 40% of Lis-LDH remains [36, 37]. The weight loss is seen in two stages in PVC and its NCs, the pyrolysis trend of Lis-LDH/PVC NCs is similar to PVC. At the first stage, the removal of moisture and highly volatile compounds are shown. The second stage is related to Lis-LDH in the range of 300–600 °C, which indicates the thermal decomposition of nanoparticle layers by removing OH groups or due to the decomposition of anionic

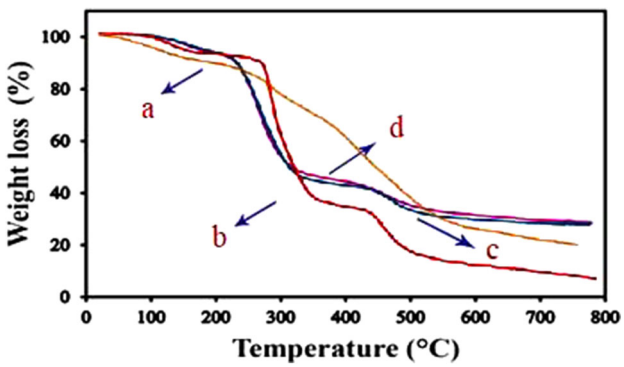

Fig. 4 Thermogravimetric analysis (TGA) curves of (a) Lis-LDH, (b) pure PVC, and (c) and (d) Lis-LDH/PVC NC 8 wt% and 12 wt%

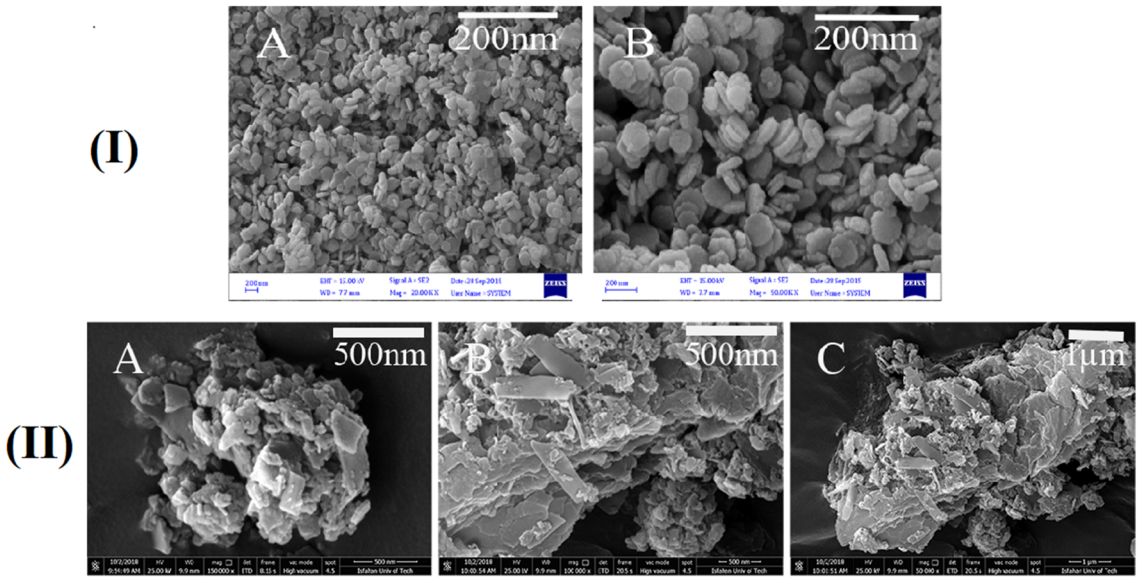

Fig. 5 FE-SEM photographs of **I** Zn/Al-LDH and **II** Lis-LDH in different magnifications

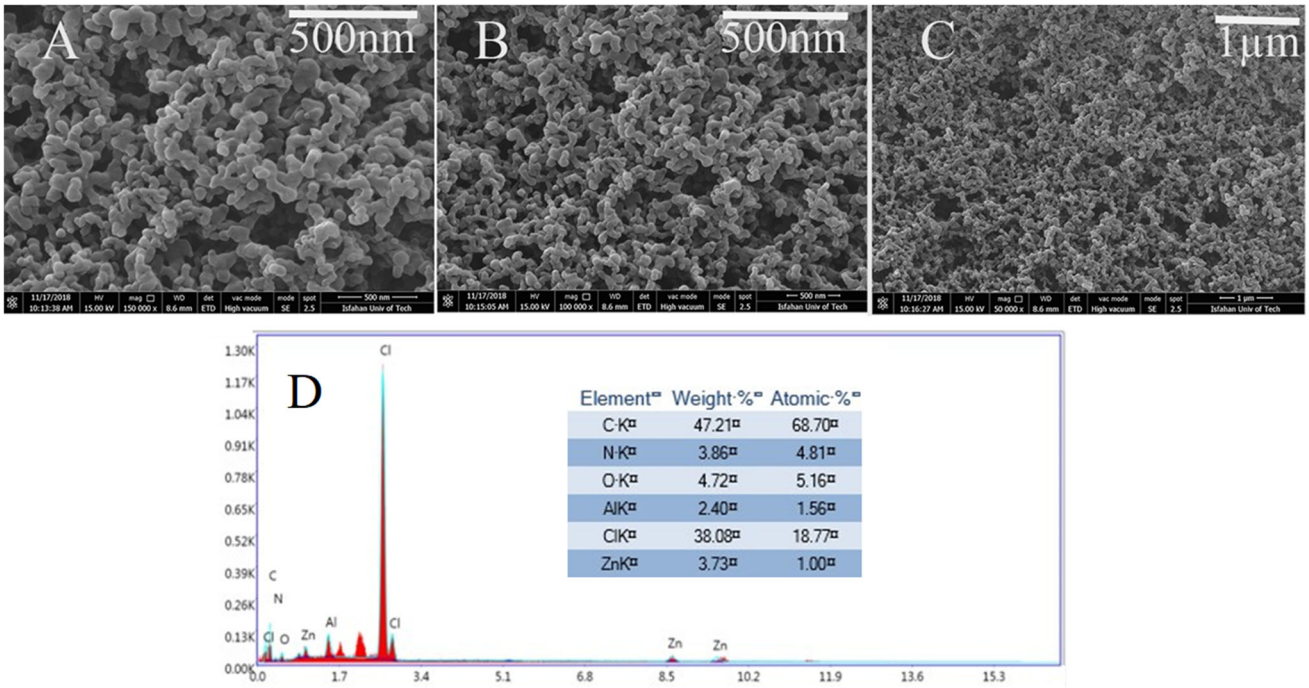

Fig. 6 **A**–**C** FE-SEM images and **D** EDAX analysis of of Lis-LDH/PVC NC 8 wt%

dye between LDH interlayers. Neat PVC has two main stages of weight loss. Despite a slight decrease in T10 and T_{50} in NCs compared to polymer, it shows that the thermal stability of PVC has increased. Char yield is usually defined as the % of solid amount you obtain at end of pyrolysis. At 800 °C, thermograms show a large increase in solid amount but as shown in Fig. 4, by adding more Lis-LDH, there is no significant difference in the amount of residual mass. Limiting oxygen index (LOI) has also been increased from 20.3 to 29.1, and these thermograms confirm that these materials are in the classification of self-extinguishing materials [38].

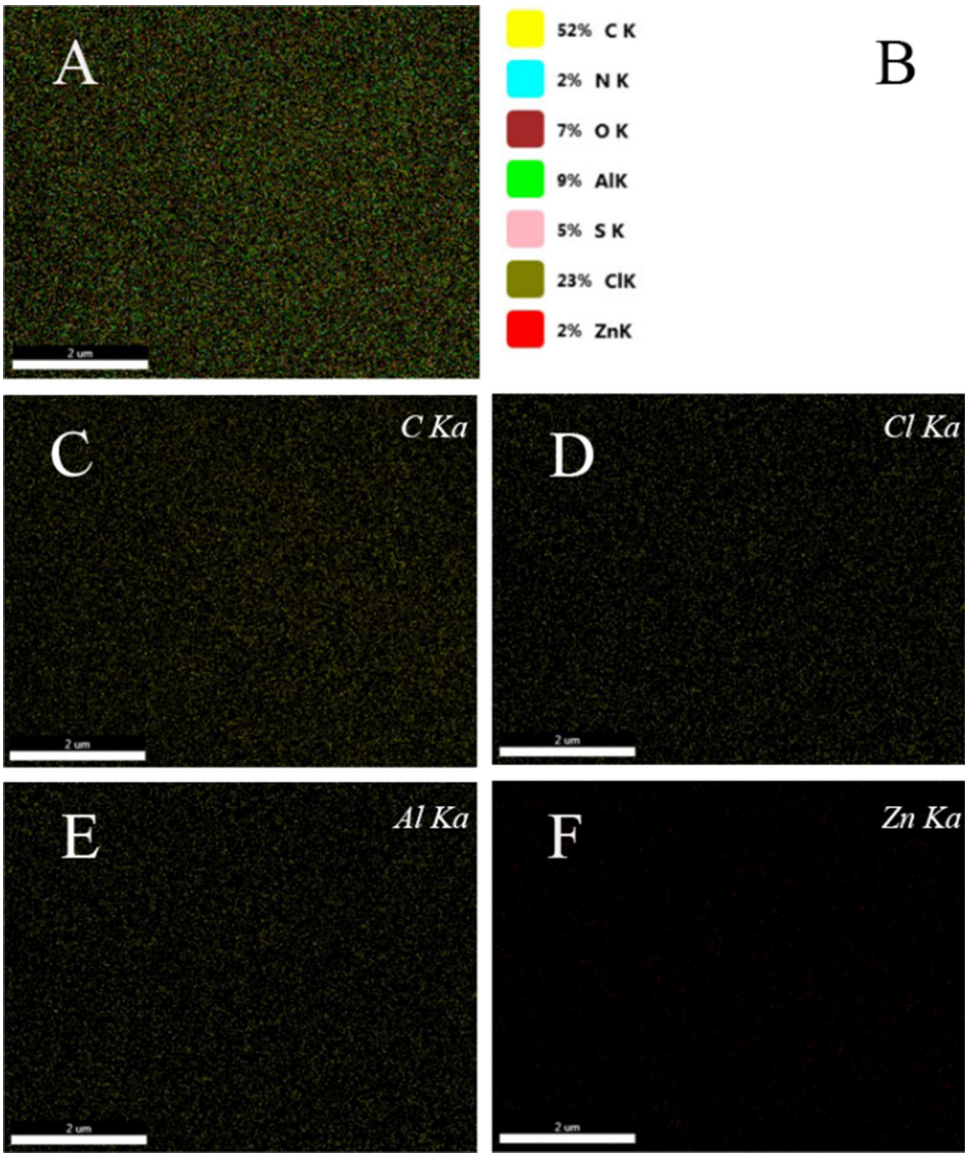

Fig. 7 EDAX mapping of Lis-LDH/PVC 8 wt% NC

3.4 Morphological study

Figure 5 shows the FE-SEM images of Lis-LDH with different magnifications. As you can see, due to the yellow color of Lissamine, the structure of Zn/Al-LDH has changed due to the growth of the Lis molecule on it and the distance between the layers has increased.

Figure 6 shows the FE-SEM images of Lis-LDH/PVC NC 8 wt%. Ethanol was added to convert the NC from film to powder. These images also show cohesive spheres and porous structures.

The EDX diagram in Fig. 7 shows the presence of Lis-LDH in the PVC polymer substrate and the dispersion diagrams of the elements. The presence of different elements and their distribution confirmed the formation of the NCs [39].

TEM was used to study the shape and size of the Lis-LDH in the PVC structure. According to Fig. 8, the size of the lamellar structure is between 27 and 30 nm. In the Lis-LDH/PVC NC 8 wt%, the particles were not agglomerated, which confirmed that Lis-LDH has a considerable effect on improving the uniform dispersion of LDH in the polymer substrate [40].

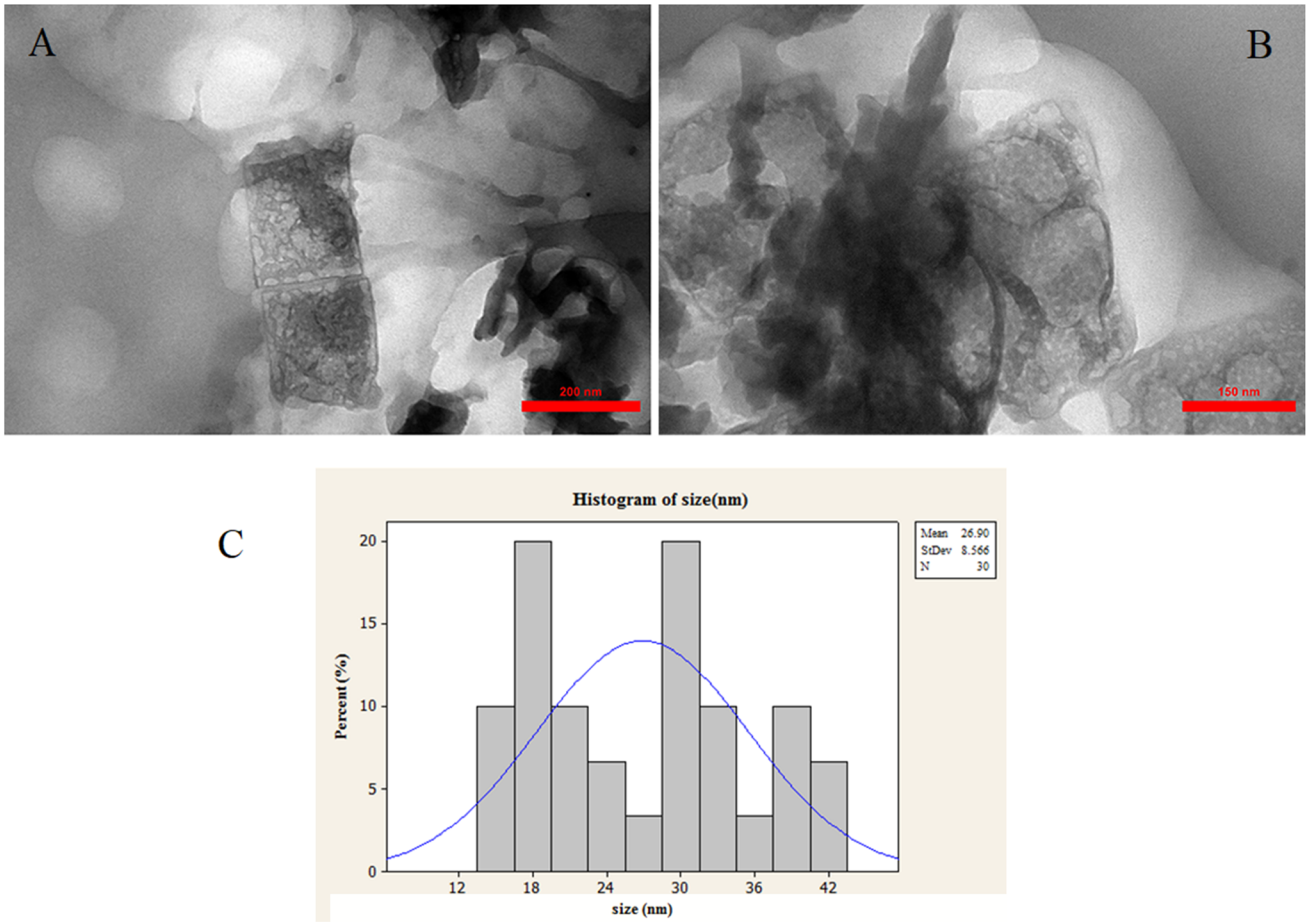

Fig. 8 **A**, **B** TEM images of Lis-LDH/PVC 8 wt% NC and **C** distribution histogram

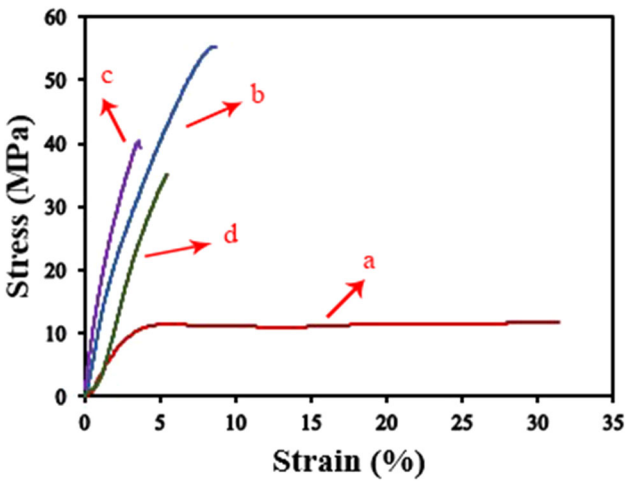

Fig. 9 Stress–strain charts of (a) Neat PVC and (b–d) the PVC NCs at room temperature

3.5 Mechanical properties

The stress–strain diagrams and mechanical properties of pure PVC and NCs composed of Lis-LDH/PVC (with various contents) are given in Fig. 9; Table 1, respectively. The presence of Lis-LDH in the polymer substrate has increased the strength and stress of the NCs up to NC 8% compared to pure polymer. This improvement in mechanical properties has been increased by increasing the percentage of nanoparticles in the polymer to 8% NC compared to pure polymer. The nanocomposite shows a 12% decrease in strength compared to the 8% sample, which can be attributed to the accumulation of nanoparticles in the polymer matrix [7, 41].

Table 1 Mechanical data of pure PVC and its NCs at room temperature

Samples	Stress (MPa)	Strain (%)	Young modulus (GPa)
Neat PVC	11.8	31.4	0.37
PVC/Lis-LDH NC 4 wt%	23.7	7.3	3.24
PVC/Lis-LDH NC 8 wt%	54.4	4.2	12.95
PVC/Lis-LDH NC 12 wt%	41.2	5.3	7.77

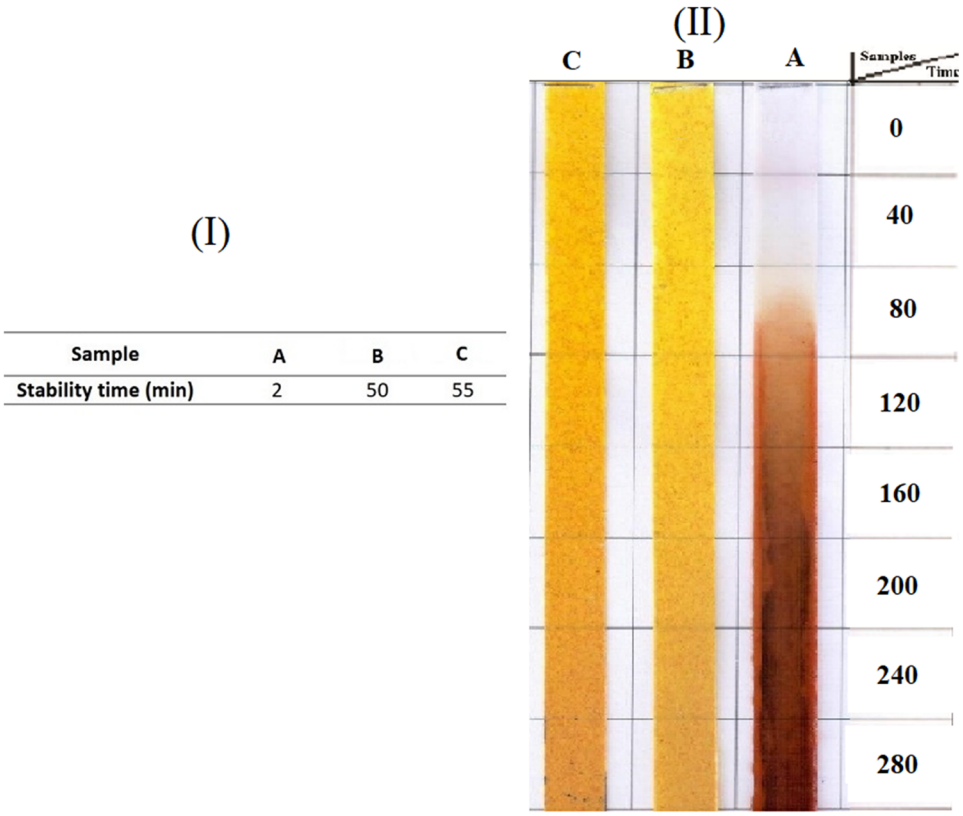

Fig. 10 **I** Congo red and **II** static thermal aging (A) control sample, (B) Lis-LDH/PVC NC 4 wt%, and (C) Lis-LDH/PVC NC 8 wt%

3.6 Congo red and static thermal aging

The results of thermal stability tests and Congo red for synthesized NCs are shown in Fig. 10. NCs were prepared according to the sample-making instructions for these tests. PVC composites containing 100 g of PVC, 20 g of dioctyl phthalate (DOP) (as the most popular plasticizer), and 4 and 8% by weight ratios of Lis-LDH were prepared by two roll mills and compared with the control sample. The NCs were exposed to 160 °C for 0–270 min. The results show that adding LDHs to the PVC/DOP composition significantly increases the thermal stability and does not discolor the PVC in the presence of heat. In the pure sample, the initial color is very clear but has started to change and darken around 90 °C. Therefore, LDHs prevent the degradation of PVC resins due to their proper interaction with chloride ions in the main PVC chain and special layer structure (Fig. 10II). In the Congo red test, the nanocomposites were placed at 180 °C. It is well known that PVC suffers from the dehydrochlorination and catalytic reaction of HCl under the influence of temperature and solar energy, which is carried out by the ionic mechanism and quickly changes the color of the Congo red detector to blue (Fig. 10I). PVC NCs containing Lis-LDH have significantly improved the thermal stability of PVC, but by adding a higher percentage of nanoparticles, no change in HCl gas emissions has been observed. LDHs prevent HCl emissions through a two-step process. In the first stage, opposing ions such as −OH of the surface of LDHs react with HCl. In the second stage, LDH itself reacts with HCl, which leads to the destruction of the structure of LDH and the formation of metal chlorides. The results of the Congo red test are consistent

with the results of static thermal stability tests. As the Congo red paper turned blue, the thermal stability test strips changed color and began to darken [4, 13, 42, 43].

4 Conclusion

To conclude this project, a new series of nanocomposite films based on PVC and nanoparticles containing zinc and aluminum LDH with the help of ultrasonic waves as an eco-friendly and fast method were prepared. It is the production of nanoparticles that both increase the heat stability of the polymer and have the ability to create dyes in the nanocomposite. The prepared nanocomposites were studied using FT-IR, XRD, and FE-SEM analysis. The FE-SEM results showed that the nanoparticles were evenly distributed within the polymer matrix. TGA results also showed improved thermal properties of nanocomposites compared to pure PVC polymer. According to the results, improvement of the tensile strength of the nanocomposites compared to the pure polymer was observed and, reciprocally, the strain decreased with increasing strength. TEM images with a magnification of 50 nm showed the lamellar structure of the nanoparticles inside the polymer substrate. It was also found that the mechanical properties of NCs increased compared to pure PVC.

Author contributions

NR contributed to software, visualization, writing and preparation of the original draft, conceptualization, validation, formal analysis, and writing, reviewing, & editing of the manuscript. ET contributed to software and writing and preparation of the original draft. MD contributed to supervision, project administration, conceptualization, validation, investigation, resources, and writing, reviewing, & editing of the manuscript.

Funding

The authors have not disclosed any funding.

Data availability

Data are available on request from the authors.

Declarations

Conflict of interest All authors declare that they have no conflict of interest.

References

1. O. Rahmanian, S. Amini, M. Dinari, J. Mol. Liq. **256**, 9–15 (2018)
2. M. Dinari, N.J. Roghani, Inorg. Organomet. Polym. Mater. **30**, 808–819 (2020)
3. S. Mallakpour, M. Dinari, Polymer **54**, 2907–2916 (2013)
4. L. Fan, L. Yang, Y. Lin, G. Fan, F. Li, Polym. Degrad. Stab. **176**, 109153 (2020)
5. S. Aisawa, C. Nakada, H. Hirahara, N. Takahashi, E. Narita, Appl. Clay Sci. **180**, 105205 (2019)
6. P.M. Pardeshi, A.K. Mungray, A.A. Mungray, Desalination **421**, 149–159 (2017)
7. Z.P. Xu, S.K. Saha, P.S. Braterman, N. D'Souza, Polym. Degrad. Stab. **91**, 3237–3244 (2006)
8. L. Ćurković, D. Ljubas, S. Šegota, I. Bačić, J. Alloys Compd. **604**, 309–316 (2014)
9. M. Li, Y.D. Liang, X. Wang, K.S. Bin, Li, X.R. Liu, Polym. Degrad. Stab. **124**, 87–94 (2016)
10. X. Zhang, L. Zhou, H. Pi, S. Guo, J. Fu, Polym. Degrad. Stab. **102**, 204–211 (2014)
11. F.J.W.J. Labuschagne, D.M. Molefe, W.W. Focke, I. Van Der Westhuizen, H.C. Wright, M.D. Royeppen, Polym. Degrad. Stab. **113**, 46–54 (2015)
12. D. Jin, S. Khanal, S. Xu, Appl. Clay Sci. **208**, 106114 (2021)
13. M. Dinari, N. Roghani, J. Polym. Res. **28**, 119 (2021)
14. M.F.H. Abd El-Kader, N.S. Awwad, H.A. Ibrahium, M.K. Ahmed, J. Mater. Res. Technol. **13**, 1878–1886 (2021)
15. A.H. Sevinç, M.Y. Durgun, Constr. Build. Mater. **300**, 123985 (2021)
16. J. Meng, B. Xu, F. Liu, W. Li, N. Sy, X. Zhou et al., Chemosphere **283**, 131274 (2021)
17. S. Shabani, M. Dinari, Inorg. Chem. Commun. **133**, 108914 (2021)
18. L. Alidokht, S. Oustan, A. Khataee, M.R. Neyshabouri, A. Reyhanitabar, Geoderma **380**, 114648 (2020)
19. O.D. Pavel, A.E. Stamate, E. Bacalum, B. Cojocaru, R. Zăvoianu, V.I. Pârvulescu, Catal. Today **366**, 227–234 (2021)
20. S.J. Song, S.W. Hyun, T.G. Lee, B. Park, K. Jo, C.S. Kim, Ecotoxicol. Environ. Saf. **205**, 111125 (2020)

21. J. Witt, J. Dietrich, S. Mertsch, S. Schrader, K. Spaniol, G. Geerling, Ocul. Surf. **18**, 901–911 (2020)
22. C.W. Lievens, Y. Norgett, N. Briggs, P.M. Allen, M. Vianya-Estopa, Contact Lens Anterior Eye **44**, 101332 (2021)
23. Z. Cheng, L. Zhang, X. Guo, X. Jiang, R. Liu, J. Taiwan. Inst. Chem. Eng. **47**, 149–159 (2015)
24. Z. Gao, L. Lu, C. Shi, X. Qian, Polym. Adv. Technol. **31**, 675–685 (2020)
25. A. Marzec, B. Szadkowski, J. Rogowski, W. Maniukiewicz, M. Kozanecki, D. Moszyński et al., J. Ind. Eng. Chem. **70**, 427–438 (2019)
26. N. Abdullah, M.H. Tajuddin, N. Yusof, Carbon-based polymer nanocomposites for dye and pigment removal, in *Carbon-Based Polymer Nanocomposites for Environmental and Energy Applications*. (Elsevier, Amsterdam, 2018), pp. 305–329. https://doi.org/10.1016/B978-0−12-813574-7.00013-7
27. N.J. Kang, D.Y. Wang, B. Kutlu, P.C. Zhao, A. Leuteritz, U. Wagenknecht et al., ACS Appl. Mater. Interfaces **5**, 8991–8997 (2013)
28. E. Abdollahi, A. Heidari, T. Mohammadi, A.A. Asadi, M. Ahmadzadeh Tofighy, Sep. Purif. Technol. **257**, 117931 (2021)
29. M. Dinari, M.A. Shirani, M.H. Maleki, R. Tabatabaeian, Carbohydr. Polym. **236**, 116070 (2020)
30. M. Dinari, S. Neamati, A. Colloids Surfaces, Physicochem. Eng. Asp **589**, 124438 (2020)
31. N.S. Al-Kadhi, Egypt. J. Aquat. Res. **45**, 231–238 (2019)
32. M. Dinari, M. Hatami, J. Environ. Chem. Eng. **7**, 102907 (2019)
33. B. Alshahrani, H.I. ElSaeedy, S. fares, A.H. Korna, H.A. Yakout, A.H. Ashour et al., Opt. Mater. **118**, 111216 (2021)
34. R. Soltani, M. Dinari, G. Mohammadnezhad, Ultrason. Sonochem. **40**, 533–542 (2018)
35. L. Ye, T. Li, L. Hong, Waste Manag. **126**, 832–842 (2021)
36. M. Dinari, R. Tabatabaeian, Carbohydr. Polym. **192**, 317–326 (2018)
37. S. Mallakpour, M. Dinari, Prog. Org. Coat. **77**, 583–589 (2014)
38. M. Dinari, H. Allami, M.M. Momeni, J. Electroanal. Chem. **877**, 114643 (2020)
39. S. Mallakpour, M. Hatami, Appl. Clay Sci. **149**, 28–40 (2017)
40. S.D. Khandare, D.R. Chaudhary, B. Jha, Mar. Pollut Bull. **169**, 112566 (2021)
41. Y. Yang, L. Xiong, X. Huang, Q. Shi, Z.W. De, Compos. Commun. **13**, 112–118 (2019)
42. R. Wen, Z. Yang, H. Chen, Y. Hu, J. Duan, J. Rare Earths **30**, 895–902 (2012)
43. J. Liu, G. Chen, J. Yang, Polymer **49**, 3923–3927 (2008)